

Energy Dissipation During Rupture of Adhesive Bonds

Alette R. C. Baljon and Mark O. Robbins

Molecular dynamics simulations were used to study energy-dissipation mechanisms during the rupture of a thin adhesive bond formed by short chain molecules. The degree of dissipation and its velocity dependence varied with the state of the film. When the adhesive was in a liquid phase, dissipation was caused by viscous loss. In glassy films, dissipation occurred during a sequence of rapid structural rearrangements. Roughly equal amounts of energy were dissipated in each of three types of rapid motion: cavitation, plastic yield, and bridge rupture. These mechanisms have similarities to nucleation, plastic flow, and crazing in commercial polymeric adhesives.

The failure of adhesive bonds is a complicated phenomenon, involving both interfacial molecular attraction and kinetic effects. The reversible work of adhesion W attributable to molecular attractions tends to be much smaller than the mechanical energy G required to break an adhesive bond. The excess work $G - W$ is dissipated during rupture. In macroscopic fracture tests on highly entangled polymeric materials, the dissipated energy can be 10^4 times greater than W (1, 2). Because G determines the strength of a structural bond, dissipation mechanisms play a dominant role in the function of adhesives. Although the kinetic effects involved in dissipation are, as yet, poorly understood (3), several key processes have been identified. Some materials form crazes: Rather than breaking along a smooth crack surface, these materials form long fibers that hold the crack faces together. The energy stored in these bridges is dissipated when they finally snap. Another source of dissipation is viscous loss in the surrounding material. In viscoelastic media, the bulk shear stress often varies as a power of the shear velocity. Gent and co-workers (1, 4) have found that the excess adhesive energy has a similar power law dependence on the rupture velocity. Roughening of the final interfaces (5) and cluster formation (3) have also been mentioned as possible sources of energy dissipation.

We have performed molecular dynamics simulations to follow the movement of individual atoms during the rupture of a thin adhesive film. These simulations provide direct information on the microscopic origins of energy dissipation and on the relative importance of different mechanisms contributing to it. Most adhesive joints fail by crack propagation. If the bounding walls are much more rigid than the adhesive film, then there is a region near the crack tip where the walls are approximately parallel and separate at constant speed. This is the

region described by our simulations. In the model (6), two rigid solid walls were joined by a thin adhesive film (Fig. 1A) consisting of linear chain molecules of 2 to 32 monomers. Monomers of mass m separated by distance r interacted through a truncated Lennard-Jones (LJ) potential (7): $V(r) = 4\epsilon[(\sigma/r)^{12} - (\sigma/r)^6]$ for $r < r_c = 2.2\sigma$. Results are presented in terms of the characteristic energy, length, and time scales ϵ (~ 30 meV), σ (~ 0.5 nm), and $\tau = \sqrt{m\sigma^2/\epsilon}$ (~ 5 ns). Adjacent monomers along each chain were also coupled through an attractive potential strong enough to prevent chain crossing and breaking (8). Each wall consisted of two (111) planes of a face-centered-cubic lattice, with the atoms coupled to lattice sites by stiff springs (6). To reduce epitaxial effects, we set the nearest neighbor spacing between wall atoms at $\sim 80\%$ of the equilibrium monomer spacing along the chain molecules. An LJ potential with modified parameters $\epsilon_{wa} = 2\epsilon$, $\sigma_{wa} = 0.9\sigma$, and $r_{wa}^c = 2.2\sigma_{wa}$ was used to model the interaction between adhesive monomers and wall atoms. The temperature was kept constant by coupling the wall atoms to a heat bath (8). All data in this report are for chains of 16 monomers, but similar results were obtained for chains of length 2 to 32.

The adhesive usually contained 2048 monomers, and each wall consisted of 800 atoms. After equilibration, we separated the walls with a uniform velocity v and monitored the particle motions, forces, potential and kinetic energies, and heat flow toward the heat bath. The adhesive energy G was obtained from the time integral of the external force applied to the moving wall.

Rupture can occur either at the wall-adhesive interface (adhesive failure) or within the adhesive film (cohesive failure). Equilibrium arguments predict that failure should occur at the interface that minimizes W , or equivalently, the final interfacial energy. Thus, cohesive failure should only occur if the adhesive completely wets the solid. Interfacial energies are difficult to

measure experimentally but could easily be determined in our simulations (9). For the results presented below, the wall-adhesive interaction was strong enough to give complete wetting, and cohesive failure was observed. Rupture creates two new adhesive-vacuum interfaces with surface tension γ , and therefore, the reversible work per unit area is $W = 2\gamma$. Contrary to equilibrium predictions, cohesive failure was also observed when the adhesive did not wet the substrate, and the work of adhesion was only weakly dependent on ϵ_{wa} . As in other systems (10), rupture occurred through nonequilibrium mechanical failure in the region with the smallest yield stress rather than where the interfacial energies were smallest. The interface has a shorter characteristic length scale and thus a larger yield stress even when the energy favors adhesive failure.

The excess work $G - 2\gamma$ exhibited the three different types of dependence on rupture velocity illustrated in Fig. 2A. These coincided with the three different regimes of shear response that have been identified in experimental studies (11) and simulations (6) of thin films. For comparison, Fig. 2B shows the mean frictional force on the top wall while moving it at a uniform shear velocity v . In the low-temperature glassy state ($T = 0.3\epsilon$), the excess work and friction approach constant values at low v . These limits correspond to the amount of adhesion hysteresis and static friction, respectively. Just above the glass transition temperature ($T = 0.6\epsilon$), both excess work and friction increase as v^x with x near $1/3$ over the range of velocities studied. At low velocities and higher temperatures ($T = 1.1\epsilon$), there is a Newtonian regime in which both quantities increase linearly with velocity.

The correspondence between the excess work and shear stress follows naturally if rupture produces smooth viscous flows in the film (1, 4). Such flows were observed at $T = 0.6\epsilon$ and 1.1ϵ , and both flow velocities and dissipation decreased to zero with v . Glassy films do not exhibit smooth flows or vanishing dissipation at low v (12, 13). Instead, rupture occurs through a sequence of rapid structural rearrangements. Moreover, shear was confined to the wall-fluid interface, whereas rupture occurred within the film.

The time dependence of rupture in glassy films is illustrated in Figs. 1 and 3. Before rupture (Fig. 1A), seven layers that span the film are visible. As the walls moved apart, the film first deformed elastically, that is, the force needed to separate the walls (Fig. 3B) and the distances between layers increased linearly with time t . During this stage, the potential energy increased, and heat flowed into the system (Fig. 3A). When the distance be-

Department of Physics and Astronomy, The Johns Hopkins University, Baltimore, MD 21218, USA.

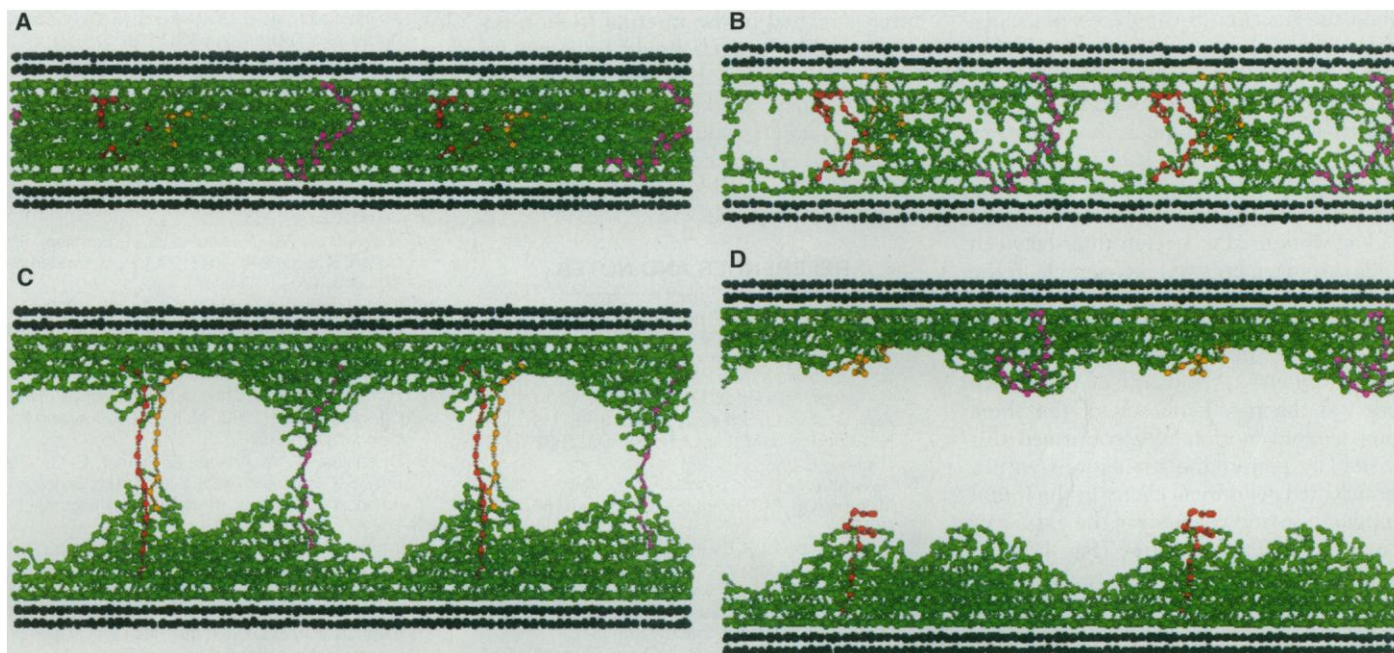


Fig. 1. Snapshots at times (A) 0τ , (B) 300τ , (C) 3100τ , and (D) 4250τ during rupture of a glassy film with temperature $T = 0.3\epsilon$ and rupture velocity $0.003\sigma/\tau$. Wall atoms are black. Most adhesive molecules are green, but the three molecules that form the final bridges have different colors. Particle

positions are projected onto the xz plane, where z (vertical) is the direction of wall separation. Periodic boundary conditions were used in the xy plane; two periodic images of each molecule along x are shown. In (B), only a thin cross section of the film is shown in order to make the cavities visible.

tween layers exceeded a threshold value, the film became unstable against density fluctuations. Small cavities formed and grew rapidly (Fig. 1B). The formation of the cavities allowed the remainder of the film to relax toward its original density and produced the sharp drop from the maximum force starting at $t = 165\tau$ in Fig. 3B. The separation at which cavities formed was independent of chain length for chains of 2 to 32 monomers. This implies that it only depends on the force between individual monomers.

Further increase in wall separation led to plastic flow. We found a sequence of sudden structural rearrangements each time the internal stress exceeded the local yield stress. The steps in the force from $t = 400\tau$ to 2000τ (Fig. 3B) coincided with these rearrangements. Between steps, the film behaved nearly elastically, and little or no energy was dissipated. For atomically smooth walls, as in Fig. 1, the unruptured portions of the film remained layered and the number of layers increased by one at each step. Similar layer-by-layer thickening has been observed in computer simulations of rupture in crystalline solids (14). To ensure that our results were not dependent on this layering phenomenon, we also performed simulations with walls whose root-mean-square roughness was greater than the layer spacing. The roughness suppressed layering, but rapid rearrangements coinciding with stepwise reductions in the force were still observed. Moreover, the excess work of adhesion was nearly unchanged.

In the late stages of rupture, the cavities had coalesced. The walls were only connected by a few bridges (Fig. 1C). The parts of chains lying within these bridges had to transmit the entire force between the walls, and they became oriented almost completely normal to the walls. The lengths of bridges grew to nearly that of a fully stretched chain. Then, one end of each chain pulled free and collapsed onto

the opposite surface. The final fractured surfaces were very rough, with pronounced bumps left by each bridge (Fig. 1D). Energy stored in the excess surface area is part of the unrecoverable work, which was gradually converted to heat as the surface annealed.

By studying hysteresis loops, we deter-

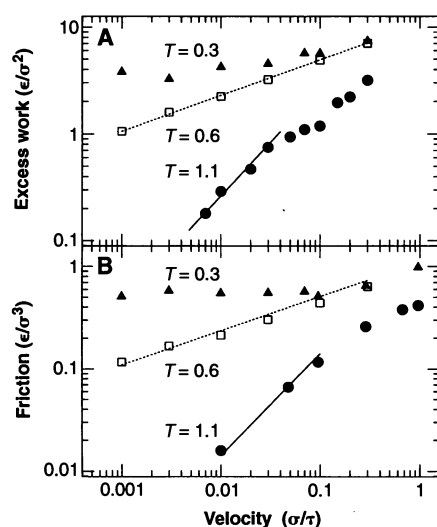


Fig. 2. (A) Excess work as a function of rupture velocity, and (B) mean frictional force on the top wall as a function of shear velocity in the (100) direction at zero pressure. Lines with slope 1/3 (dashed) and 1 (solid) indicate the power law scaling observed at $T = 0.6\epsilon$ and 1.1ϵ , respectively. Variations between runs were less than the symbol size.

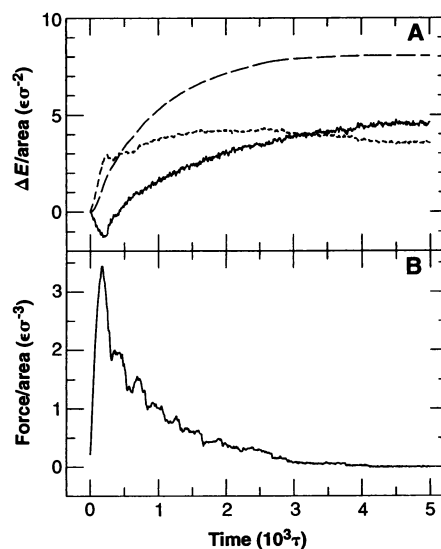


Fig. 3. Time dependence of (A) energy changes ΔE and (B) the force on the walls during rupture of the glassy film shown in Fig. 1. Lines in (A) indicate the external work (dashed), the potential energy increase (dotted), and the total heat flow (solid). Because the mean kinetic energy remains constant at fixed T , the work equals the sum of the potential energy change and heat flow.

mined the fraction of the excess work dissipated during each of the three types of rapid motion: cavitation, plastic yield, and bridge rupture. Starting from any wall separation, one can cycle the walls outward by a given amount and then back to the initial separation. The total work done to perform such a cycle is equal to the energy dissipated. The work used to stretch films between rapid rearrangements was recoverable in the low-velocity limit. In contrast, each rapid rearrangement led to an amount of dissipation that was nearly independent of the rupture velocity. About 1/3 of the excess work was dissipated in each of the three types of rapid motion. We confirmed this division by performing simulations with a pre-nucleated cylindrical cavity in the initial configuration and calculating the extra surface area after bridge rupture (Fig. 1D).

Processes usually become reversible as the velocity decreases. The reason that the dissipation remained constant in glassy films was that they were always far from equilibrium during rapid rearrangements (3). Instantaneous velocities reached large values that were set by the yield stress of the glass rather than by the mean rupture velocity. Similar instabilities may be the origin of static friction in solid-on-solid sliding (15). Motion through rapid rearrangements was also observed at higher temperatures, particularly cavitation and bridge rupture. However, in this case the dissipation was velocity-dependent, and viscous dissipation dominated at low velocities.

In our simulations, the adhesive energy G for glassy films was approximately twice the reversible work. Comparable ratios have been measured in experiments on tightly cross-linked rubber on glass (16) and on adsorbed monolayers of short molecules (17). The latter studies have also shown that adhesion hysteresis becomes negligible when the adhesive enters a fluid state (Fig. 2). Ratios between G and W are orders of magnitude larger for commercial adhesives. Although they have much larger chain lengths and film thicknesses, these adhesives exhibit the same types of rapid yield events that are seen in our simulations, namely cavity nucleation, plastic flow, and stringing or crazing (1, 2, 13). We found that all of these processes dissipated more energy with increased film thickness and chain length. For example, the size of bridges and the amount of work done to stretch them grew linearly with chain length for lengths between 8 and 32 monomers. Somewhat larger chains should become entangled (8) and allow the formation of the extremely long bridges observed in crazes. Entanglement would also enhance viscous losses. Energy dissipated during plastic flow increased with the thickness of the flowing region and with the local yield stress. The

latter is related to the internal friction between molecules and should be larger for realistic molecules than for our smooth chains. It may also be increased by introducing liquid crystalline order or hydrogen bonds between molecules. Both are present in silk, which is well known for its superior mechanical properties (18).

REFERENCES AND NOTES

1. D. Maugis, in *Adhesion and Friction*, M. Grunze and H. Kreuzer, Eds. (Springer-Verlag, Berlin, 1990).
2. R. P. Wool, *Polymer Interfaces: Structure and Strength* (Hanser, Munich, 1995).
3. K. Kendall, *Science* **263**, 1720 (1994).
4. A. N. Gent and J. Schultz, *J. Adhes.* **3**, 281 (1972); A. N. Gent and S.-M. Lai, *J. Polym. Sci. B* **32**, 1543 (1994).
5. S. A. Joyce, R. C. Thomas, J. E. Houston, T. A. Michalske, R. M. Crooks, *Phys. Rev. Lett.* **68**, 2790 (1992).
6. P. A. Thompson, G. S. Grest, M. O. Robbins, *ibid.*, p. 3448; P. A. Thompson, M. O. Robbins, G. S. Grest, *Isr. J. Chem.* **35**, 93 (1995).
7. M. P. Allen and D. J. Tildesley, *Computer Simulation of Liquids* (Clarendon, Oxford, 1987).
8. K. Kremer and G. S. Grest, *J. Chem. Phys.* **92**, 5057 (1990).
9. J. G. Kirkwood and F. P. Buff, *ibid.* **17**, 338 (1949); P.

- A. Thompson, W. B. Brinckerhoff, M. O. Robbins, *J. Adhes. Sci. Technol.* **7**, 535 (1993).
10. J. N. Israelachvili and A. Berman, *Isr. J. Chem.* **35**, 85 (1995).
11. S. Granick, *Science* **253**, 1374 (1991); G. Reiter, A. L. Demirel, S. Granick, *ibid.* **263**, 1741 (1994).
12. P. H. Mott, A. S. Argon, U. W. Suter, *Philos. Mag. A* **68**, 537 (1993).
13. H. H. Kausch, Ed. *Crazing in Polymers* (Springer-Verlag, Berlin, 1983).
14. U. Landman, W. D. Luedtke, N. A. Burnham, R. J. Colton, *Science* **248**, 454 (1990); R. M. Lynden-Bell, *ibid.* **263**, 1704 (1994).
15. G. A. Tomlinson, *Philos. Mag.* **7**, 905 (1929); J. N. Glosli and G. McClelland, *Phys. Rev. Lett.* **70**, 453 (1993).
16. K. Kendall, *J. Adhes.* **7**, 55 (1974).
17. H. Yoshizawa, Y.-L. Chen, J. N. Israelachvili, *J. Phys. Chem.* **97**, 4128 (1993); M. K. Chaudhury and M. J. Owen, *ibid.*, p. 5722.
18. D. Kaplan, W. W. Adams, B. Farmer, E. C. Viney, Eds. *Silk Polymers* (ACS Symposium Series 544, American Chemical Society, Washington, DC, 1994).
19. We thank P. A. Thompson, G. S. Grest, P. M. McGuiggan, and J. N. Israelachvili for useful discussions. Support from National Science Foundation grant DMR-9110004, Petroleum Research Fund grant 28790-AC5,9, and the Pittsburgh Supercomputing Center is gratefully acknowledged.

18 August 1995; accepted 15 November 1995

The Structure and Stability of Atomic Liquids: From Clusters to Bulk

Jonathan P. K. Doye and David J. Wales

Insights into the structure of simple liquids are presented from analysis of the effect of the range of interatomic forces on the multidimensional potential energy surfaces of bulk material and clusters. An understanding at the microscopic level is provided of how the liquid phase is destabilized in systems with very short-range interparticle forces. For small clusters bound by long-range interatomic forces, the lowest energy minimum has an amorphous structure typical of the liquidlike state. This suggests an explanation for the transition from electronic to geometric magic numbers (structures of special stability) observed in the mass spectra of sodium clusters.

The phase diagrams of simple substances depend sensitively on the form of the interatomic or intermolecular forces (1). In particular, the range of temperature for which a liquid-vapor transition can occur as a function of pressure decreases with the range of attraction (2). For example, the interparticle forces of some colloids (3) and perhaps C_{60} (4) have such a short range that no liquid phase is observed—instead, there is only a single fluid phase. In contrast, the critical temperature for sodium is about seven times as large as the triple-point temperature because of the long-range interatomic forces. Here, we provide an understanding of this phenomenon at the microscopic level and relate it to structural models of liquids and glasses. Because these models often make use of results from cluster studies (5,

6), we consider finite clusters as well as bulk material. By understanding how the behavior of clusters is similar to or different from that of bulk material, we can address questions concerning the evolution of the

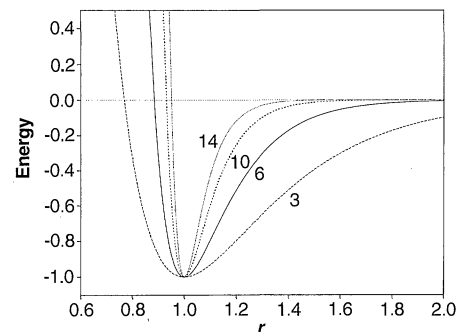


Fig. 1. The Morse potential for different values of the range parameter ρ_0 as marked. Quantities in all figures are in reduced units.

University Chemical Laboratories, Lensfield Road, Cambridge CB2 1EW, UK.